NONDESTRUCTIVE STRUCTURAL DAMAGE DETECTION IN FLEXIBLE SPACE STRUCTURES USING VIBRATION CHARACTERIZATION

Final Report

NASA/ASEE Summer Faculty Fellowship Program - 1991

Johnson Space Center

Prepared By:	James M. Ricles, Ph.D.
Academic Rank:	Assistant Professor
University & Department:	University of California, San Diego Department of AMES, 0411 La Jolla, California 92093
NASA/JSC	
Directorate:	Engineering
Division:	Structures and Mechanics
Branch:	Loads and Structural Dynamics
JSC Colleague:	David A. Hamilton
Date Submitted:	August 16, 1991
Contract Number:	NGT-44-001-800

ABSTRACT

Spacecraft are susceptible to structural damage over their operating life from impact, environmental loads, and fatigue. Structural damage that is not detected and not corrected may potentially cause more damage and eventually catastrophic structural failure. NASA's current fleet of reusable spacecraft, namely the Space Shuttle, has been flown on several missions. In addition, configurations of future NASA space structures, e.g. Space Station Freedom, are larger and more complex than current structures, making them more susceptible to damage as well as being more difficult to inspect. Consequently, a reliable structural damage detection capability is essential to maintain the flight safety of these structures. Visual inspections alone can not locate impending material failure (fatigue cracks, yielding), it can only observe post-failure situations. An alternative approach is to develop an inspection and monitoring system based on vibration characterization that assesses the integrity of structural and mechanical components.

A methodology for detecting structural damage is presented. This methodology is based on utilizing modal test data in conjunction with a correlated analytical model of the structure to: (1) identify the structural dynamic characteristics (resonant frequencies and mode shapes) from measurements of ambient motions and/or force excitation, (2) calculate modal residual force vectors to identify the location of structural damage, and (3) conduct a weighted sensitivity analysis in order to assess the extent of mass and stiffness variations, where structural damage is characterized by stiffness reductions. The approach is unique from other existing approaches in that varying system mass and stiffness, mass center locations, the perturbation of both the natural frequencies and mode shapes, and statistical confidence factors for structural parameters and experimental instrumentation are all directly accounted for.

An analytical assessment was conducted on the methodology. The results of this assessment show the method to provide a precise indication of both the location and the extent of structural damage.

INTRODUCTION

Flexible space structures, launch vehicles, and satellites are susceptible to structural damage over their operating lifes from impact, operating loads, and fatigue. Undetected and uncorrected damage can lead to structural deterioration of their members and consequently jeopardize the flight safety of the structure. Thus, numerous damage inspection methods and monitoring procedures have been developed and used by NASA and the aerospace industry. These include: X-ray; ultrasonic testing; magnetic resonance; coin tap; dye penetrate; and visual inspection. These methods can be time consuming and are local assessments, often requiring the exposure of structural elements to the inspector and equipment for detecting damage. As a monitoring system for detecting spacecraft in orbit (i.e. Space Station Freedom) none of these are appropriate. An alternative approach, which formed the basis for the study reported herein, is to recognize the fact that modal vibration test data (structural natural frequencies and mode shapes) characterizes the state of the structure [Ewins, 1984]. Therefore, postflight and inflight (e.g. monitoring) data can be utilized to distinguish whether changes (damage) have occurred to the structure by comparing this data to a set of baseline data. Modal testing as a means of inspection has several advantages. Direct exposure of structural elements is not required, while at the same time more of the complete structure can be inspected in one modal test by having appropriately placed sensors. The consequences of this is a reduction in schedule and cost.

In the past, the purpose of performing modal testing on a structure has been to correlate and calibrate the structure's analytical model in order that the mode shapes and frequencies of the model and test results agree over selected frequency ranges. Correcting analytical models in this manner is often referred to as system identification (SID). A vast amount of work has been done in the area of SID and procedures have evolved for application in the industry. In order to use SID in damage detection, the formulation must be based on maintaining element connectivity. Some of the SID methods which qualify and have been extended to damage detection are those of Kabe [1985] and Chen and Garba [1988]. Both of these however are based on the severe limitation that the mass is constant and changes in vibration characteristics are associated with only stiffness loss or gain. Some of the more recent development in damage detection by vibration characterization is that of Stubbs [1990], which accounts for the possibility of change of mass and/or stiffness. The development however ignores the sensitivity to mode shape perturbation. All of the above noted methods do not consider uncertainty in instrumentation.

This study was concerned with developing a new methodology for nondestructive damage detection in flexible space structures, in which the phenomena ignored in current methods are accounted for. The methodology was formulated on the basis of using modal test data to characterize the state of the structure, considering: varying system mass and stiffness; mass center locations; perturbation in vibration frequencies and mode shapes; statistical weighting factors for analytical model structural parameters (e.g. element mass and stiffness); and confidence factors for errors in experimental instrumentation. The scope of this study included implementing the damage detection methodology onto a computer in order to validate and assess the approach. This validation and assessment effort is based on analytically derived modal test data for a number of different cases, representing damage scenarios involving two structures. The theoretical basis of the methodology and summary of its assessment is included in this report. Conclusions based on the assessment and topics for future research are noted.

THEORETICAL BASIS

General

The algorithm for damage detection is given in Fig. 1, and consisting of three main parts: 1) Modal Test Survey; 2) Locating Damage; and 3) Assessing the Severity of Damage. In the modal test survey a baseline experimental modal test is performed to measure the vibration properties Λ_0, which includes natural frequencies ω_0 and mode shapes Φ_0. This data is used to

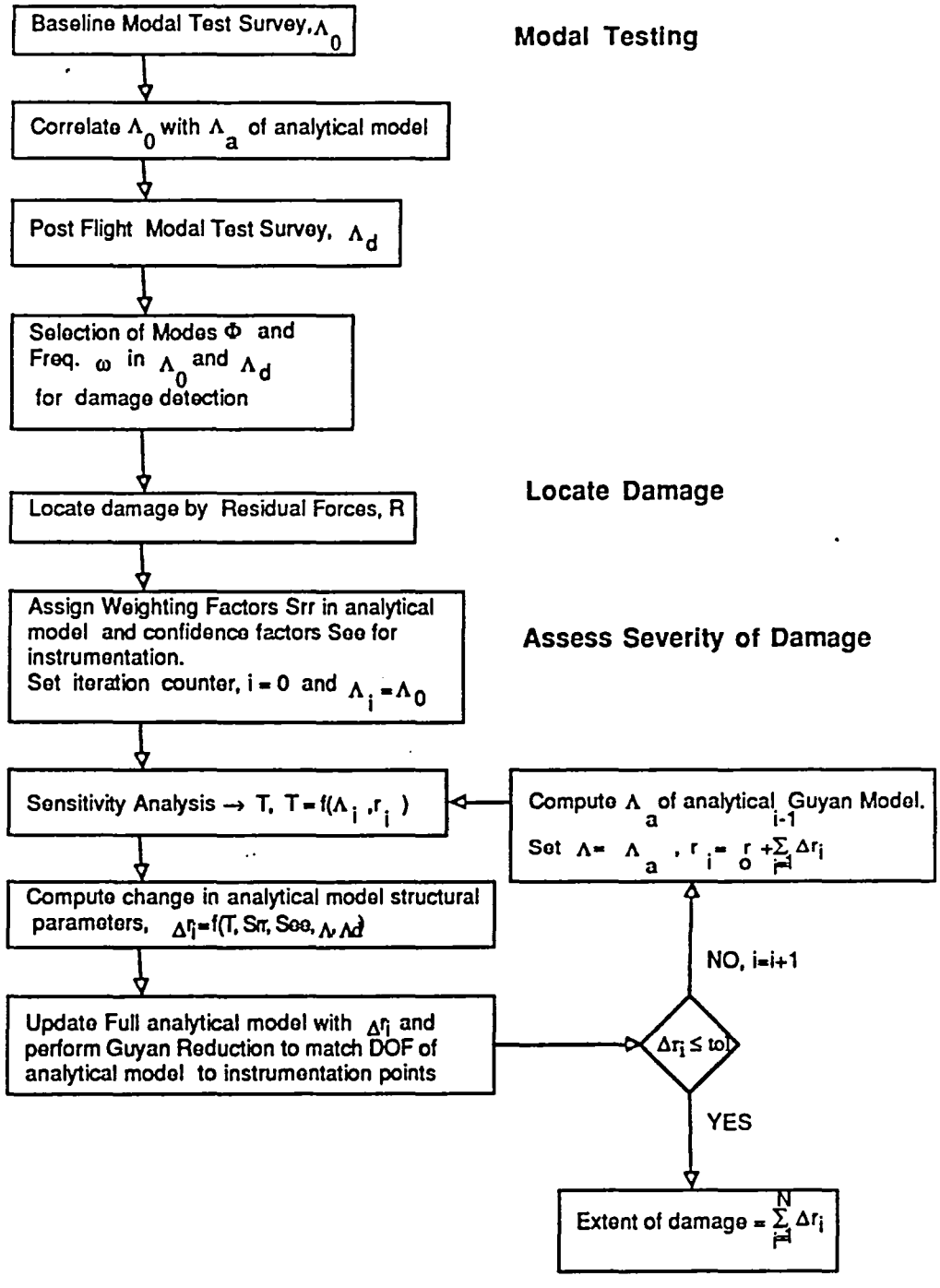

Figure 1. - Damage Detection Algorithm

correlate with an analytical model and set the baseline for subsequent comparison in the remaining parts of the algorithm. The modal test survey is completed by conducting postflight, or inflight for monitoring, experimental modal testing to measure the vibration properties Λ_d , which includes natural frequencies ω_d and mode shapes Φ_d.

It is necessary to select appropriate frequencies and mode shapes in Λ_o and Λ_d to start the damage detection. This is accomplished by considering the correlation of Λ_o with the vibration properties Λ_a of the analytical model. The selection of modes must be done such that discrepancies between Λo and Λa are smaller than those of Λ_o and Λ_d, otherwise one will be incorrectly estimating the damage due to the fact that the analytical model is corrected to match Λ_o and further undergoes changes towards Λ_d . The selection of modes should be based on the following criteria: a smaller frequency shift $\Delta\omega$ as well as a superior set of values for modal assurance criterion (MAC) between Λ_o and Λ_a compared to Λ_o and Λ_d , and an adequate cross orthogonality check (COR) between Λ_o and Λ_a ; where for mode i (considering Λ_o and Λ_a)

$$\Delta\omega_i = (\omega_i)_0 - (\omega_i)_a \qquad [1]$$

$$MAC_i = \frac{\left[\sum_{j=1}^{N} (\phi_{ji})_0 (\phi_{ji})_a\right]^2}{\sum_{j=1}^{N} (\phi_{ji})_0^2 \sum_{j=1}^{N} (\phi_{ji})_a^2} \qquad [2]$$

and for all modes , $$COR = \Phi_0^T M_a \Phi_a \qquad [3]$$

in which M_a = analytical mass matrix, and j = instrumentation point location. In Eqns [1], [2], and [3] the assessment for Λ_o - Λ_d is performed by replacing Λ_a with Λ_d.

Locating Damage

Identifying the location of damage in the structure is based on differences in Λ_d and Λ_0 through an extended application of the Residual Force Method [Chen and Wang, 1988]. In concept, the experimental frequencies and mode shapes must satisfy an eigenvalue equation, where considering the damaged structure and mode i

$$(K_d - \lambda_{di} M_d)\phi_{di} = 0 \qquad [4]$$

in which K_d and M_d are the experimental (unknown) stiffness and mass matrices associated with the damaged structure, respectively, and λ_{di} (ω_{di}^2) the experimental measured eigenvalue (natural frequency squared) corresponding to the experimental measured mode shape ϕ_{di} of mode i of the damaged structure. Assuming that the damaged stiffness and mass matrices are defined as

$$K_d = K_b + \Delta K \qquad [5]$$

$$M_d = M_b + \Delta M \qquad [6]$$

in which K_b , M_b = known baseline stiffness and mass matrices of the analytical model, and ΔK, ΔM = unknown changes in stiffness and mass matrices due to damage. Substituting Eqns. [5] and [6] into Eqn. [4] and rearranging, one arrives at the definition of the residual force vector R_i for mode i

$$R_i = -\left(\Delta K - \lambda_{d_i}\Delta M\right)\phi_{d_i} \qquad [7a]$$

$$= \left(K_b - \lambda_{d_i}M_b\right)\phi_{d_i} \qquad [7b]$$

where the right hand side of Eqn. [7b] is known and will be equal to zero for an undamaged structure. By examining R_i, where each term corresponds to a measurement point on the structure, one can locate regions in the structure that are damaged. These locations correspond to the degrees-of-freedom (DOF) that have large magnitudes in R_i. It should be emphasized that one should calculate R_i for several modes, for if a damaged member is near a node line where the modal displacement is near zero, the residual forces will have a tendency to be near zero.

Assessment of Damage Severity

The assessment of damage severity is based on establishing a relationship between the measured vibration characteristics and structural parameters (members mass, stiffness, section geometry) in the damaged region using a first order Taylor series expansion:

$$\Lambda_d = \Lambda_0 + T(r_d - r_0) + \varepsilon \qquad [8]$$

where Λ_d , Λ_0 = arrays containing corresponding selected measured natural frequencies and modes shapes in which $\Lambda^T=\{\omega^2,\Phi\}^T$; r_d, r_0 = unknown array of structural parameters in damaged region and known baseline array of structural parameters in same location of structure, ε = array of testing errors associated with each measured parameter (e.g. mode shape amplitudes and natural frequencies). Matrix T is a sensitivity matrix that relates the change in vibration parameters, accounting for the perturbation in natural frequencies and mode shapes:

$$T = \begin{bmatrix} \frac{\partial\omega^2}{\partial K} & \frac{\partial\omega^2}{\partial M} \\ \frac{\partial\Phi}{\partial K} & \frac{\partial\Phi}{\partial M} \end{bmatrix}_0 \begin{bmatrix} \frac{\partial K}{\partial r} \\ \frac{\partial M}{\partial r} \end{bmatrix}_0 \qquad [9]$$

The subscript "o" is associated with the baseline configuration. The four individual submatrices in the first matrix of T represents partial derivatives of the eigenvalues and mode shapes with respect to the coefficients of the stiffness and mass matrices, whereas the second matrix of T represents the partial derivatives of the stiffness and mass matrices with respect to the structural parameters r. The derivatives of the eigenvalues and mode shapes are determined from the measured baseline data Λ_0 and analytical mass matrix, where for mode k and considering instrumentation points i and j it can be shown:

$$\frac{\partial\omega_k^2}{\partial K_{ij}} = \frac{\phi_{ik}\phi_{jk}}{\phi_k^T M\phi_k}; \qquad \frac{\partial\phi_{rk}}{\partial K_{ij}} = \sum_{n=1}^{q}\left[\frac{\phi_{in}\phi_{jk}\phi_{rn}}{(\omega_k^2 - \omega_n^2)\phi_n^T M\phi_n}\right](1 - \delta_{nk}) \qquad [10]$$

$$\frac{\partial \omega_k^2}{\partial M_{ij}} = \frac{-\omega_k^2 \phi_{ik}\phi_{jk}}{\phi_k^T M \phi_k} \quad ; \quad \frac{\partial \phi_{rk}}{\partial M_{ij}} = \sum_{n=1}^{q} \left[\frac{-\omega_k^2 \phi_{in}\phi_{jk}\phi_{rn}(1 - \delta_{nk})}{(\omega_k^2 - \omega_n^2)\phi_n^T M \phi_n} - \frac{\phi_{in}\phi_{jk}\phi_{rn}\,\delta_{nk}}{2\,\phi_n^T M \phi_n} \right] \qquad [11]$$

in which q = number of retained modes in Λ_0 for the assessment, n = index to identify mode number.

The goal in the assessment is to determine r_d. This is accomplished by first treating the difference $R = r_d - r_0$ for all structural parameters as normally distributed random variables with a zero mean and a specified covariance S_{RR} in order to deal with the uncertainty in the damage assessment. Treating the test measurement error also as a random variable with a zero mean and specified covariance $S_{\varepsilon\varepsilon}$ leads to the solution, where it can be shown that

$$r_d = r_o + S_{RR}^* T^T [T S_{RR}^* T^T + S_{\varepsilon\varepsilon}]^{-1} (\Lambda_d - \Lambda_0) \qquad [12]$$

where

$$S_{RR}^* = S_{RR} - S_{RR} T^T [T S_{RR} T^T + S_{\varepsilon\varepsilon}]^{-1} T S_{RR} \qquad [13]$$

Values for the diagonal terms (e.g. variances) in S_{RR} are assigned in conjunction with the results of the residual force analysis, all off diagonal terms being set equal to zero. Only those members suspected of damage are given nonzero variances, and therefore are the only members that are emphasized in the damage severity assessment. In this study all suspected members with damage were given equal variances. It should be noted that uncertainties in the analytical model can also be considered by assigning nonzero variances related to the structural parameters associated with these uncertainties.

If the relationship between the stiffness and mass components and the structural system is linear the method will converge in one step. However, the partial derivatives of the eigenvalues with respect to the stiffness and mass coefficients is nonlinear if enough damage has occurred to cause a frequency shift, as illustrated in Fig 2(a). To obtain a more accurate assessment of the severity of damage it is necessary to either continuously monitor the system (inflight damage monitoring) or use the correlated analytical model to update the damage assessment in order to converge to Λ_d, as illustrated in Fig. 2(b). Each update involves completing the tasks associated with the part of the algorithm labelled Damage Severity Assessment in Fig. 1. The change in the structural parameters at the i^{th} updating point is $\Delta r_i = r_d - r_i$, where r_d comes from Eqn. [12] considering $r_0 = r_i$ with $T = T_i$ and $\Lambda_0 = \Lambda_i$. Here r_i = the current value for the structural parameters, which reflects the accumulated changes from previous updates and T_i = the sensitivity matrix based on the vibration characteristics of the updated baseline analytical model (or in the case of an online monitoring system, the measured characteristics at the point). Convergence is achieved when Δr_i during an update becomes less than the tolerance for convergence, with the predicted extent of damage equal to the sum of Δr_i for all of the update cycles, as indicated in Fig 2(b).

As noted in the damage detection algorithm (Fig. 1) the full analytical model is updated, which may likely have more degrees-of-freedom (DOFs) than instrumented DOFs of the modal test structure. Guyan reduction is therefore required to reduce the model's DOFs to the instrumentation points. The other alternative is to maintain the full model in the assessment and not evaluate the columns in T pertaining to non-instrumented DOFs. The first procedure was pursued. In evaluating the sensitivity matrix, the derivatives of the stiffness and mass coefficients involves the Guyan transformation matrix Ψ:

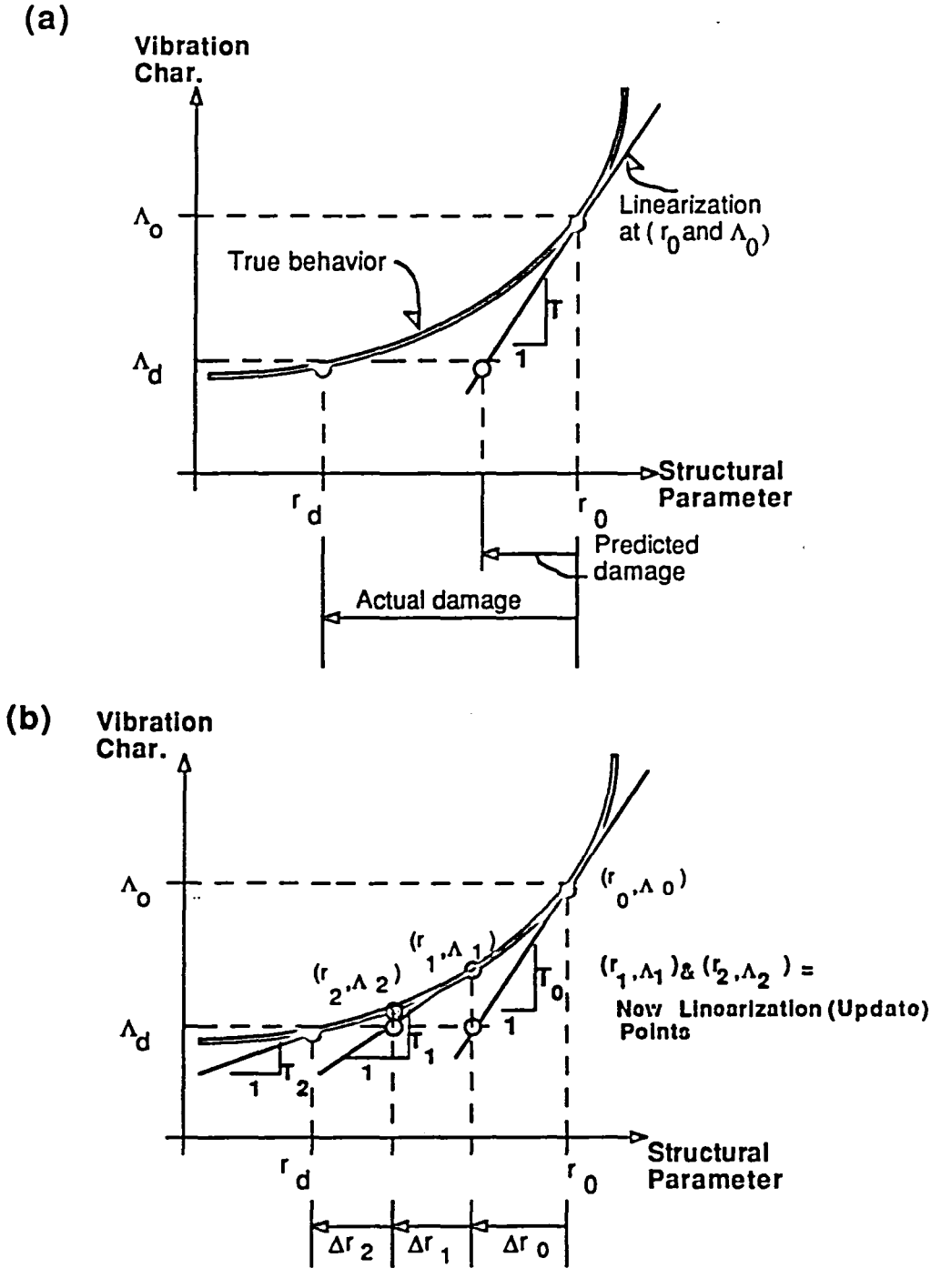

Figure 2. - (a) Linearization of the Nonlinear Relationship and, (b) Updating to Obtain Convergence.

$$\frac{\partial K_{ij}}{\partial r} = \frac{\partial}{\partial r}\left(\Psi^T K^* \Psi\right) = \frac{\partial \Psi^T}{\partial r} K^* \Psi + \Psi^T \frac{\partial K^*_{ij}}{\partial r} \Psi + \Psi^T K^* \frac{\partial \Psi}{\partial r} \qquad [14]$$

$$\frac{\partial M_{ij}}{\partial r} = \frac{\partial}{\partial r}\left(\Psi^T M^* \Psi\right) = \frac{\partial \Psi^T}{\partial r} M^* \Psi + \Psi^T \frac{\partial M^*_{ij}}{\partial r} \Psi + \Psi^T M^* \frac{\partial \Psi}{\partial r} \qquad [15]$$

where K^* and M^* = stiffness and mass matrices related to the full analytical model.

VALIDATION AND ASSESSMENT

Program of Investigation

The verification and assessment of the damage detection methodology involved an 'analytical modal test structure', and therefore is analytical in nature. An experimental assessment is planned as a future study. The analytical assessment involved imposing damage to the modal test structure and 'forgetting' where these locations existed and the extent of imposed damage. An attempt was then made to detect the damage, using Λ_0 based on the undamaged 'analytical modal test modal' and Λ_d based on the damaged 'analytical modal test model'.

Two structures were considered in this study: Structure A and Structure B. Both of these structures are shown in Fig. 3. Structure A consists of a 40 member truss structure with 32 in plane translational DOF. All DOF are located at the nodes shown in Fig. 3, having lumped mass of m. At two nodes a greater mass of M was assigned. Each of these additional mass represented 36% of the total structural mass and were placed to represent similar situations that exists in space truss type structures. All 32 DOF were assumed to be instrumented, hence the ensuing analytical model (which was a finite element model- FEM) used in the algorithm shown in Fig. 1 represented a perfectly correlated model where $\Lambda_0 = \Lambda_a$. Structure B had similar geometry as Structure A, except that the mass was more distributed and in plane rotational and translational DOF existed, which resulted in a 168 DOF structure with 80 elements. The nodes, each having a lumped mass, and elements is shown in Fig. 3(b). Only 32 translational DOF of Structure B were instrumented, and identified in Fig. 3(c). The FEM used to assess the damage was a Guyan reduced FEM, where the full FEM had the 168 DOF of the modal test model. Thus, Λ_a was based on a 32 DOF Guyan reduced FEM, with Λ_0 and Λ_d obtained from the 168 DOF modal test model (modal displacements being only 'known' at the 32 instrumented translational DOF).

A total of five cases were studied, each representing a different damage scenario. These cases are described in Table 1, and refer to damaged members shown in Fig. 3. In all cases $S_{\varepsilon\varepsilon}$ was based on standard deviations equal to 2% of the modal frequencies and maximum modal displacements of each mode retained in the assessment. Members suspected of damage were weighted equally, S_{RR} based on standard deviations of 15% of the baseline material's Young modulus.

Structure A

The natural frequency of vibration for the first six modes of Structure A are given in Table 2. The baseline frequencies, f_0, are identical to the FEM frequencies f_a since both were produced from the same analytical model. Thus no MAC or orthogonality checks were required. The damaged frequencies f_d pertaining to the postflight modal test for all cases and the shift from the baseline frequency f_0 are also given in Table 2. The amount of frequency shift is considered small. For mode 2 of Case 1 and mode 1 of Case 2 there is no frequency shift due to damage. In Case 2 the damaged structural frequencies become larger due to the combined effect of decrease in stiffness and decrease in mass (5% of M). As more members are damaged without loss of mass (Cases 3 and 4) there is a greater frequency shift, for the f_d for these cases becomes smaller.

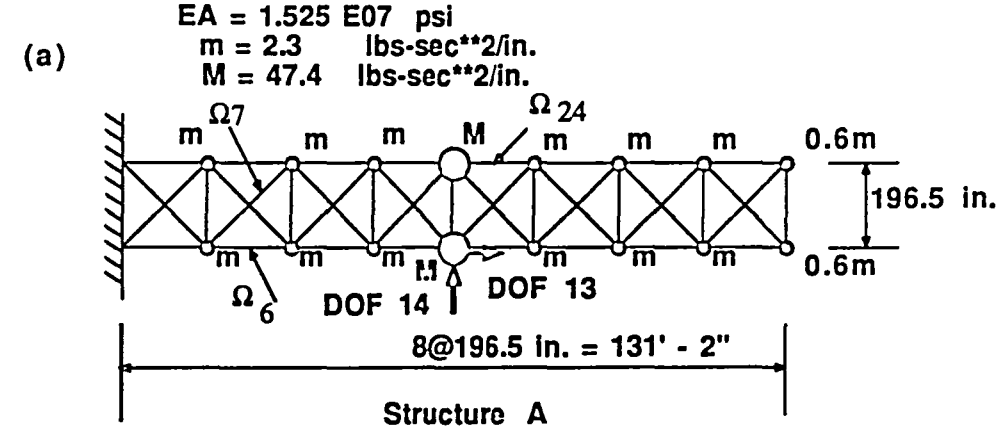

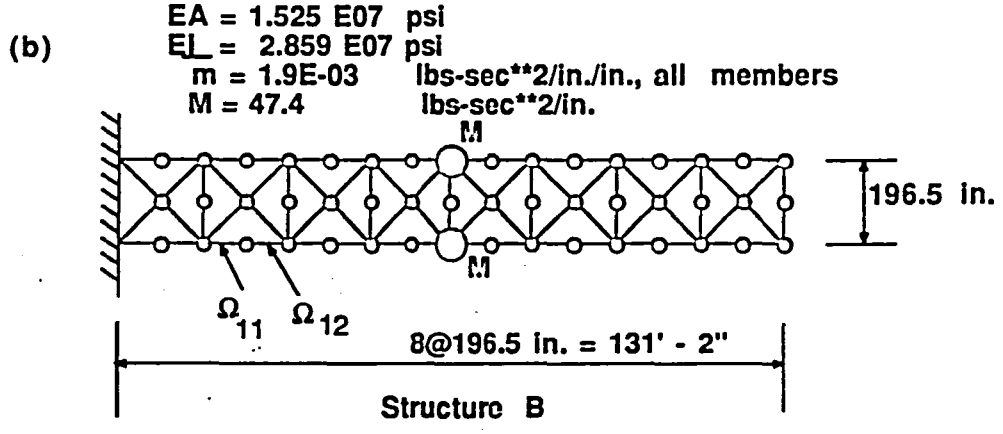

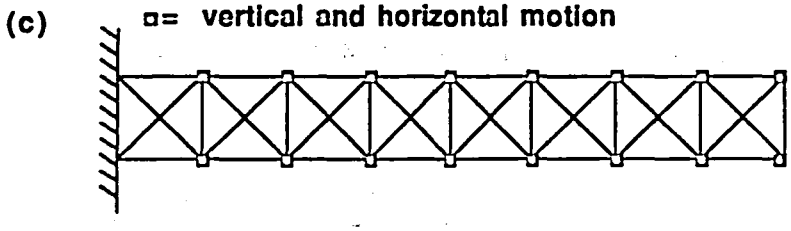

Figure 3. - (a) Modal Test Structure A, (b) Structure B, and (c) Instrumentation Points.

TABLE 1. - Case Studies for Assessment

Case	Structure	Comments
1	A	10% stiffness loss in member (Ω_6)
2	A	10% stiffness loss in member, (Ω_6), 5% loss of mass at DOF 13 &14
3	A	two members with stiffness loss, $(\Omega_6 = 10\%; \Omega_7 = 5\%)$
4	A	3 members with stiffness loss, $(\Omega_6 = 10\%; \Omega_7 = 5\%; \Omega_{24} = 5\%)$
5	B	10% stiffness loss in one member, (Ω_{11})

TABLE 2. - Case Studies for Assessment, Structure A

Mode	Natural Frequency - Hz.									
	f_0	f_a	Case 1		Case 2		Case 3		Case 4	
			f_d	$f_0 - f_d$	f_d	$f_0 - f_d$	f_d	$f_0 - f_d$	f_d	$f_0 - f_d$
1	0.499	0.499	0.496	0.003	0.499	0.0	0.496	0.003	0.496	0.003
2	2.212	2.212	2.212	0.000	2.222	-0.010	2.211	0.001	2.204	0.008
3	3.144	3.144	3.126	0.018	3.157	-0.013	3.125	0.019	3.125	0.019
4	7.109	7.109	7.105	0.004	7.157	-0.048	7.101	0.008	7.078	0.031
5	9.815	9.815	9.814	0.001	9.932	-0.117	9.814	0.001	9.808	0.007
6	11.646	11.646	11.638	0.008	11.649	-0.003	11.635	0.011	11.630	0.016

TABLE 3. - Natural Frequencies and Modal Assurance Criteria, Structure B

Mode	Natural Frequency - Hz.					MAC	
	f_0	f_a	f_d	$f_0 - f_a$	$f_0 - f_d$	$\phi_0; \phi_a$	$\phi_0; \phi_d$
1	0.554	0.555	0.552	-0.001	0.002	0.999	0.999
2	2.704	2.706	2.704	-0.002	0.000	0.999	0.999
3	3.313	3.315	3.304	-0.002	0.009	0.999	0.998
4	7.827	7.921	7.826	-0.094	0.001	0.997	0.996

The residual forces for mode 1 are shown in Fig. 4 for all cases. The forces were calculated using Eqn. [7b], where K_b and M_b are that of the FEM. The residual forces acting at the nodes for which no value is given in Fig. 4 were 3 to 4 orders of magnitude smaller than those shown. The residual forces for Case 1 give a clear indication than member 6 is damaged, for the forces are equal and opposite and act at the ends of member 6. For Case 2 the residual forces again give an indication that member 6 is damaged, and that there exists some change at DOF 13 and 14 which is associated with the location of the loss of mass. The residual forces for Case 3 indicate damage in members 6 and 7, by recognizing the way in which the forces balance. Likewise, the residual forces for Case 4 give an indication that members 6, 7,and 24 are damaged. The forces for mode 1 appear to also correctly indicate the relative extent of damage among the members. This is generally not true, for damaged members near a node line will have a small residual force due to the small modal displacements at these locations.

The results of the assessment of damage severity are shown in Fig. 5, where the predicted damage in terms of percent of baseline value is plotted as a function of number of updates. All results show convergence to the exact result and give a precise indication of the severity of member damage. The affect of retaining a larger number of modes in the assessment is to increase the rate of convergence, as evident in Case 1 which compare the results using the first 2 modes with that using the first 4 modes. Cases 2 and 3 both used the first 4 modes and Case 4 the first 6 modes. In Case 4, using only the first 4 modes resulted in a slow rate of convergence. For all cases S_{RR} was used in lieu of S_{RR}^* in Eqn [12], and therefore remained a constant. It was found that using S_{RR}^* in Eqn [12] as defined by Eqn. [13] resulted in a slower rate of convergence with no improvement in the final result.

Structure B

The natural frequencies for the first 4 modes of Structure B are given in Table 3. The major shift in frequency due to damage is shown to occur in mode 3, where the difference in the baseline f_0 and postflight (damaged) frequencies f_d is 0.009 Hz. The accuracy of the Guyan reduced FEM used as the analytical model in the assessment is shown to be very good in the first three modes. However, the FEM's frequency of f_a = 7.921 Hz. for the 4^{th} mode shows a significant discrepancy ($f_0 - f_a$) compared to the frequency shift due to damage ($f_0 - f_d$) . Modes higher than the 4^{th} mode were found to have an even greater discrepancy between f_0 and f_a . It is therefore advisable to include only the first 3 modes in the assessment of damage. The values for the MACs are also given in Table 3. Good correlation exist between the mode shapes of the first 4 modes of the baseline and analytical FEM, as well as the baseline and postflight modal test data. The cross orthogonality check between the FEM and measured baseline data is summarized in Table 4. It is apparent that the 4^{th} mode of the baseline data does not have good orthogonality with respect to the FEM modes, as reflected in the value of 0.795 on the diagonal and 0.028 on the off diagonal.

The residual forces of mode 1 are shown in Fig. 6. Forces at nodes not shown are 3 to 4 orders of magnitude smaller than those shown. The residual forces indicate that damage has occurred in either both or one of the elements between the residual forces (element 11 and 12). It was determined that damage had occurred only in element 11 by noting that the residual forces of Fig. 6 diminish when assigning a nonzero variance only to this member and proceeding with one update in the damage severity assessment. When assigning nonzero variances to both elements 11 and 12 the residual forces increased after performing one update. The assessment for damage severity thus preceded with a nonzero variance assigned only to element 11.

The results of the severity of damage assessment are shown in Fig. 7. The curve labeled Guyan III corresponds to using the first 4 modes, Guyan II the first 3 modes, and Guyan I the hypothetical situation of a perfectly correlated FEM with respect to the first 4 modes (e.g. Λ_a

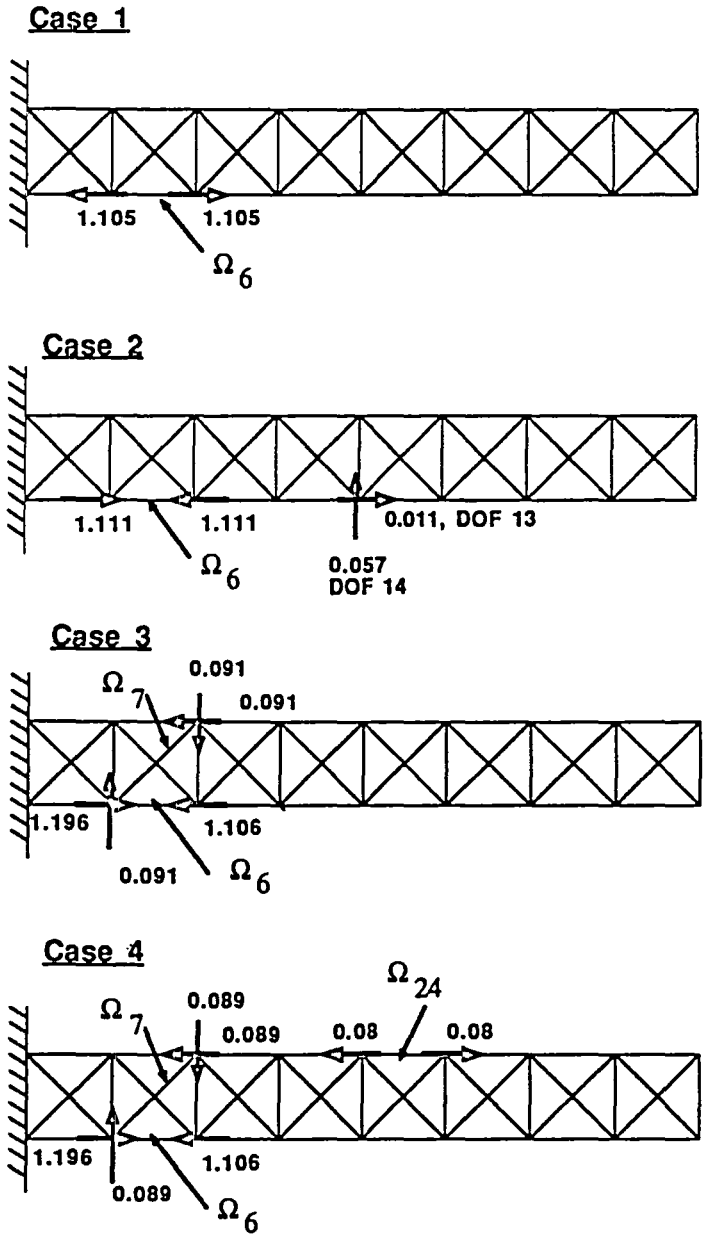

Figure 4. - Mode 1 Residual Forces for Structure A.

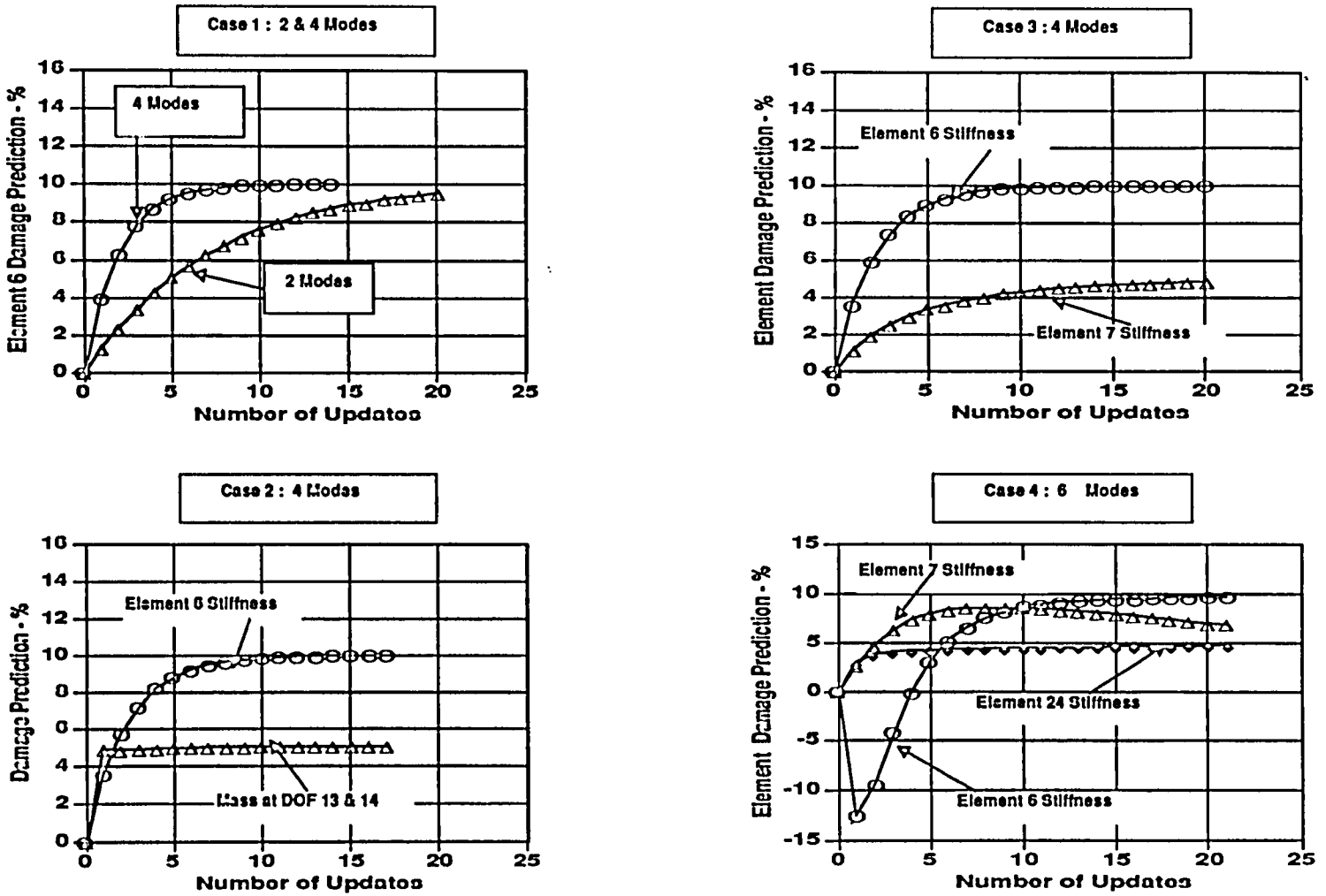

Figure 5. - Structure A Damage Assessment Results

TABLE 4. - Cross Orthogonality Check, Structure B

Test $\phi 0$ \ FEM ϕa	Mode	1	2	3	4
	1	0.999	0.001	0.001	0.011
	2	-0.004	0.999	0.003	0.008
	3	0.003	0.006	0.990	0.009
	4	0.013	0.028	0.015	0.795

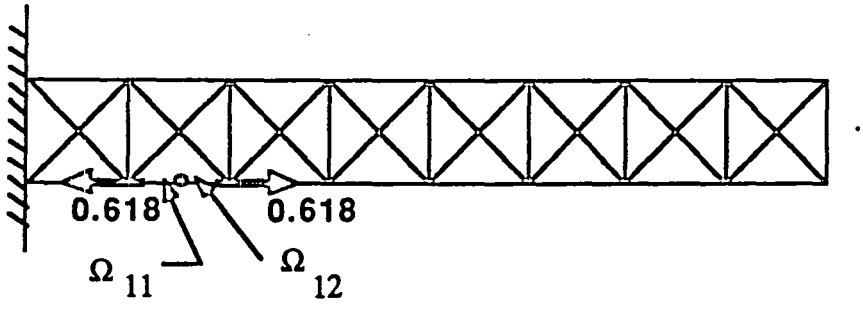

Figure 6. - Mode 1 Residual Forces for Structure B, Case 5.

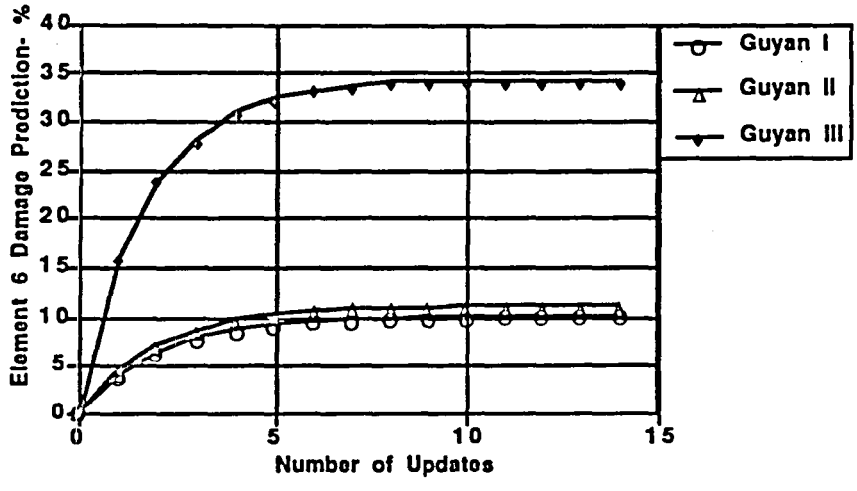

Figure 7. - Structure B Damage Assessment Results

= Λ_0). The results for Guyan I converge to the exact result of 10%, while Guyan converges to 11% and Guyan to 34%. It is apparent that the 4^{th} mode is causing the method to over predict the severity of damage in member 11 by correcting for discrepancies between Λ_a and Λ_0 in addition to assessing the extent of damage. As noted above, mode 4 was determined not to be fit for inclusion in the assessment; indicating the importance of performing and examining the results of the correlation analysis before performing the damage assessment for severity. In the event that not enough modes are correlated, one could use the damage assessment algorithm to first correct the analytical model, using λ_0 and ϕ_0 in Eqn. [7b] to locate areas in the FEM needing adjustment and using the vibration characteristics for Λ_0 and Λ_a instead of Λ_0 and Λ_d in Eqn [12] to determine the necessary correction for the FEM.

As a final comment, the differences in f_0 and f_d are small as well as those of f_0 and f_a, and in the practical sense less than the resolution of most modal testing equipment. It would be expected in a real application involving modal testing that the differences between f_0 and f_d would be greater as well as those between f_0 and f_a. The results of this study are still considered valid since it is the relative differences between $f_0 - f_d$ and $f_0 - f_a$ that are important.

CONCLUSIONS

Based on the results of this study involving a two step procedure of detecting damage and assessing its severity the following conclusions are noted:

1. The method of detecting locations of structural damage by the Residual Force Method gives good results.

2. Basing the assessment for severity of damage on suspected members, as found by the Residual Force Method, can result in an accurate assessment. The correlation of the analytical model used in the assessment algorithm with the baseline data is important. The use of frequency shift, modal assurance criteria, and cross orthogonality checks appear to give good guidance on retaining correct modes in the damage assessment for severity and minimizing the error.

Areas which are suggested for further study include:

1. An experimental verification of the methodology for detecting damage.

2. A further investigation involving the calibration of the above criteria for selecting which modes should be retained in the assessment for damage.

3. Use of the methodology to simultaneously perform system identification and assessment for damage for analytical models that are not well correlated with the baseline data.

4. Use of the method as an online damage monitoring system for large space structures such as Space Station Freedom.

Work is currently continuing in the these areas which have been suggested as needing further study.

REFERENCES

1. Chen, J.C. and Garba, J.A., "On-Orbit Damage Assessment for Large Space Structures," AIAA Journal, Vol. 26, No. 12, June 1988.

2. Chen, T.Y. and Wang. B.P., "Finite Element Model Refinement Using Modal Analysis Data," *Proceedings of AIAA/ASME 29th Structures, Structural Dynamics, and Materials Conference*, April 1988.

3. Ewins, D. J., " Modal Testing: Theory and Practice," John Wiley and Sons, Inc., 1984.

4. Kabe, A.M. " Stiffness Matrix Adjustment Using Mode Data," *AIAA Journal*, Vol. 23, No. 9, Sept. 1985.

5. Stubbs, N., T. Broone and R. Osegueda, "Nondestructive Construction Error Detection in Large Space Structures," *AIAA Journal*, Vol. 28, No. 1, 1990.